CrossMark

Tylvalosin exhibits anti-inflammatory property and attenuates acute lung injury in different models possibly through suppression of NF-κB activation

Zhanzhong Zhao [a,b,1,*], Xiangfang Tang [a,1], Xinghui Zhao [b,*], Minhong Zhang [a], Weijian Zhang [c], Shaohua Hou [a], Weifeng Yuan [a], Hongfu Zhang [a], Lijun Shi [a], Hong Jia [a], Lin Liang [a], Zhi Lai [d], Junfeng Gao [d], Keyu Zhang [e], Ling Fu [b], Wei Chen [b,*]

[a] State Key Laboratory of Animal Nutrition, Department of Veterinary Medicine, Beijing Institute of Animal Husbandry and Veterinary Medicine, Chinese Academy of Agricultural Sciences, No. 2 Yuanmingyuan West Road, Haidian District, Beijing 100193, People's Republic of China
[b] Beijing Institute of Biotechnology, No. 20 Dongdajie Street, Fengtai District, Beijing 100071, People's Republic of China
[c] Shanghai Municipal Animal Innocuous Treatment Center, No. 50 Lane 4088, Puwei Road, Fengxian District, Shanghai 201415, People's Republic of China
[d] Biopharmavet Institute, No.161 Zhenye Road, Songjiang District, Shanghai 201619, People's Republic of China
[e] Key Laboratory for Veterinary Drug Safety Evaluation and Residue Research, Department of Pharmacy, Shanghai Veterinary Research Institute, Chinese Academy of Agricultural Sciences, No. 518 Ziyue Road, Minhang District, Shanghai 200241, People's Republic of China

ARTICLE INFO

ABSTRACT

Tylvalosin, a new broad-spectrum, third-generation macrolides, may exert a variety of pharmacological activities. Here, we report on its anti-oxidative and anti-inflammatory activity in RAW 264.7 macrophages and mouse treated with lipopolysaccharide (LPS) as well as piglet challenged with porcine reproductive and respiratory syndrome virus (PRRSV). Tylvalosin treatment markedly decreased IL-8, IL-6, IL-1β, PGE2, TNF-α and NO levels in vitro and in vivo. LPS and PRRSV-induced reactive oxygen species (ROS) production, and the lipid peroxidation in mice lung tissues reduced after tylvalosin treatments. In mouse acute lung injury model induced by LPS, tylvalosin administration significantly attenuated tissues injury, and reduced the inflammatory cells recruitment and activation. The evaluated phospholipase A2 (PLA2) activity and the increased expressions of cPLA2-IVA, p-cPLA2-IVA and sPLA2-IVE were lowered by tylvalosin. Consistent with the mouse results, tylvalosin pretreatment attenuated piglet lung scores with improved growth performance and normal rectal temperature in piglet model induced by PRRSV. Furthermore, tylvalosin attenuated the IκBα phosphorylation and degradation, and blocked the NF-κB p65 translocation. These results indicate that in addition to its direct antimicrobial effect, tylvalosin exhibits anti-inflammatory property and attenuates acute lung injury through suppression of NF-κB activation.

© 2014 Elsevier Inc. All rights reserved.

1. Introduction

Acute lung injury (ALI) and its more severe form, acute respiratory distress syndrome (ARDS), major causes of respiratory failure with high morbidity and mortality, are observed under multiple pathogenic conditions, among which are sepsis, gastric acid aspiration, major trauma, repeated transfusions and infections with influenza A virus H5N1 and severe acute respiratory syndrome coronavirus (SARS-CoV) [1–3]. ALI affects more than 200,000 people in the US each year, with approximately 75,000 deaths, making it an important cause of morbidity, mortality, and health care expenditure [4]. Although extensive investigation explored some pathogenetic factors of ALI, the effect of various approaches to treat disease remains limited because of the

complex process of development of ALI [5]. To date, the underlying mechanism of ALI remains elusive and no effective regimen is available. The only one treatment that definitely improves survival involves reducing the volume of air applied to the lungs during mechanical ventilation [1]. Thus, new strategies are still required for achieving effective treatment of ALI, which might ultimately aid the clinical therapy for patients with ALI/ARDS.

ALI and ARDS are characterized by an intense pulmonary inflammatory response, involving polymorphonuclear neutrophils (PMNs) recruitment, interstitial edema, a disruption of epithelial integrity, and lung parenchymal injury [3]. The pathogenesis of ALI/ARDS involves disorders of oxidant/anti-oxidant and inflammation/anti-inflammation, the upregulation of adhesion molecules, and the increased production of chemokines [6,7]. Activated PMNs contribute to lung injury by releasing inflammatory cytokines, proteolytic enzymes, ROS and other proinflammatory mediators which display key events in ALI and may represent a potential target for therapy. Inflammatory cytokines, such as interleukin 1β (IL-1β), IL-8, and IL-6, play a major role in mediating and amplifying ALI/ARDS by stimulating chemotaxis and activation of neutrophils [3,9]. Pharmacotherapies aimed at blocking a specific cytokine, such as IL-1 or TNF-α, have been unsuccessful [10], which suggest that a more global inhibition of cytokine signaling network may be required to impede lung injury. Therefore, it is very important to develop novel therapeutic approaches to modulating the balance between pro-inflammatory and anti-inflammatory response and restoring immune homeostasis. In addition, alveolar epithelial cell function and barrier integrity are crucial to preserve normal gas exchange, and injury or loss of epithelial cells may lead to progression of ALI/ARDS [3,11]. In all, understanding of the mechanisms in the development of ALI/ARDS is essential for developing novel therapeutic options to treat this syndrome.

Animal modeling experiments of ALI have been very useful in providing some directions into the mechanisms related to disease pathogenesis, and providing opportunities to explore new and innovative therapeutic targets. Therefore, different animal models of experimental lung injury have been developed. Mouse models of ALI could be established by intraperitoneal (i.p.), tracheal (i.t.) or intranasal (i.n.) instillation of LPS, ventilator, or smoking inhalation in mice. LPS is an important component of the cell walls of gram-negative bacteria, which is often used to establish the experimental model of ALI [12]. ALI represents a state of excess production of inflammatory mediators, including cytokines, chemokines, and adhesion molecules [8]; and the LPS is a major stimulus for release of these mediators, which may further cause pulmonary damage leading to ALI [3]. Although great advances in understanding the

pathophysiology of ALI had been achieved, the available therapies have not reduced the mortality or increased the quality of life in survivors.

Although many studies focusing on the pathophysiology of ALI have been done in rodent, rodents are different from humans in many ways, especially with regard to lung anatomy and the behavior of inflammatory mediators or cytokines. Small animal models, though useful for large-scale economical screening of new methods, have limitations and may not be directly relevant to clinical conditions. However, larger animals are more useful for detailed studies over a longer period and are essential before clinical trials can be performed [13]. Compared with other species, pigs and humans show remarkable anatomical, physiological and immunologically similarity [14], which are useful experimental animals to study ALI. Humans share the same symptoms as pigs, including fever, metabolic dysfunctions, systemic hypotension, pulmonary hypertension, vascular leakage resulting in lung edema, and increased proinflammatory cytokines, including IL-1β and TNF-α [15]. Likewise, disseminated intravascular coagulation (DIC) and similar end-organ failure are observed in the pig and in humans. Also, pigs are gentle, easy to feed, and show higher survival rates. Domestic pigs have a significantly lower cost in China. These facts support the idea that the pig can serve as an excellent animal model to study the pathogenesis of ALI or ARDS. In addition, the pig has attracted attention as a valuable preclinical model for medical research. PRRSV is a member of the family Arteriviridae, order Nidovirales, that replicates in lung alveolar macrophages and induces several cytokines including IL-6, IL-8, IL-10, and TNF-α involving pulmonary inflammation response [16,17], producing an influenza-like illness associated with respiratory distress [18] in young piglets. Therefore, PRRSV-induced respiratory distress in piglet may be a novel and safe animal model to study ALI, since this virus is not a zoonotic pathogen unlike SARS-CoV or H5N1.

Tylvalosin (Fig. 1) is a new broad-spectrum, third-generation macrolides, which is a tylosin derivative with the modification of 3-acetyl-4′-isovaleryl (acetylisovaleryltylosin tartrate) and its molecule weight is 1042. Like other macrolide compounds, this drug is being increasingly recognized to possess a broad spectrum of biological activities and important therapeutic applications [19,20]. However, the detailed mechanism of anti-inflammatory and immunomodulation activities of tylvalosin is unclear. To address these issues, the current study was designed to investigate the effects of tylvalosin on LPS-stimulated RAW 264.7 macrophages, as well as on LPS and PRRSV-induced ALI and explore the underlying mechanisms responsible for its activity.
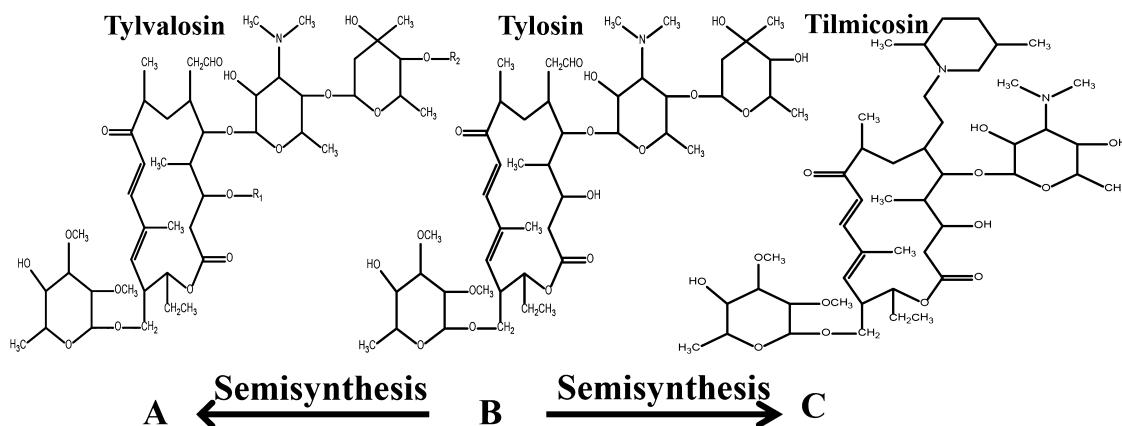

Fig. 1. Chemical structure of tylosin, tylvalosin (Tyl), and tilmicosin (Til). In tyl, R1 is acetyl, and R2 is isovaleryl.

2. Materials and methods

2.1. Chemicals and reagents

Tylvalosin ($\geq$90%) [20] was provided by Eco Animal Health (London, United Kingdom). Tilmicosin, LPS (*Escherichia coli* 055:B5), 3-(4,5-dimethylthiazol-2-y1)-2,5-diphenyltetrazolium bromide (MTT), *N*-(1-naphthyl)-ethylenediamine dihydrochloride, sulfanilamide and 7′-dichlorofluorescein-diacetate (DCFH$_2$-DA) were purchased from Sigma Chemical Co. (St. Louis, MO, USA). The PLA2 substrate 1-*O*-(6-dabcyl-aminohexanoyl)-2-*O*-(12-(5-BODIPYentanoyl)aminododecanoyl)-sn-glyceryl phosphatidylcholine (DBPC) was from Echelon Bioscience (Salt Lake City, UT, USA). Dulbecco's modified Eagle's medium (DMEM), Fetal bovine serum (FBS), penicillin and streptomycin for cell culture use were obtained from Invitrogen-Gibco (Grand Island, NY, USA). Mouse TNF-α, IL-1β, IL-8 IL-6 and PGE2 enzyme-linked immunosorbent assay (ELISA) kits were purchased from R&D Systems (Minneapolis, MN, USA) and Cayman Chemicals (Ann Arbor, MI, USA). The myeloperoxidase (MPO) and malondialdehyde (MDA) detection kits were provided by Jiancheng Bioengineering Institute of Nanjing (Nanjing, Jiangsu Province, China). Rabbit mAb p-IκBα, mouse mAb IκBα, rabbit mAb p-cPLA2, HRP-conjugated goat anti-rabbit, goat anti-mouse and donkey anti-goat antibodies were purchased from Cell Signaling Technology (Beverly, MA, USA). Mouse mAb iPLA2, rabbit mAb cPLA2 and goat mAb sPLA2 were from Santa Cruz Biotechnology (Santa Cruz, CA, USA). All other chemicals were of reagent grade.

2.2. Cells and virus

The RAW 264.7 macrophage cell line, obtained from the American Type Culture Collection (ATCC, Rockville, MD), was maintained in DMEM supplemented with 10% heat-inactivated FBS, 3 mM glutamine, antibiotics(100 U/ml penicillin and 100 U/ml streptomycin) at 37 °C under a humidified atmosphere of 5% CO$_2$. Cells at passages 10–20 were used for the experiments. In all experiments, macrophages were incubated in the presence or absence of various concentrations of tylvalosin or tilmicosin, which were always added 1 h prior to LPS (1 μg/ml) treatment.

PRRSV isolation strains (An, Fj, Hb, Gx, Hn and Jx), grown on Marc-145 cells (4th passage) were used in this study. Marc-145 cells were cultivated in DMEM supplemented with 10% heat-inactivated FBS, 3 mM glutamine, antibiotics (100 U/ml penicillin and 100 U/ml streptomycin) at 37 °C under a humidified atmosphere of 5% CO$_2$ and used for PRRSV production and titration.

2.3. Animals

Female ICR mice, weighing approximately 18 to 20 g, were purchased from the Vital River Laboratory Animal Technology Co., Ltd (Beijing, China). The mice were housed in microisolator cages and received food and water ad libitum. The laboratory temperature was 24 $\pm$ 1 °C, and relative humidity was 40–80%. Mice were housed for 7 days to adapt the environment before experimentation.

Three-week-old crossbred piglets from a herd free of PRRSV and with no measurable PRRSV serum antibody titers were obtained from commercial farms, housed in isolated rooms at the animal facilities and were under the supervision of a veterinarian. Throughout the duration of the study, all animals received food and water ad libitum. The piglets were numbered by ear-tagging and acclimatized for 1 week before experiments.

All laboratory personnel and animal caretakers involved with the study were blinded to the treatments given to the respective groups. All animal experiments were approved by the Animal Care and Use Committee of the Beijing Institute of Animal Husbandry and Veterinary Medicine, China Academy of Agricultural Sciences, Beijing, and performed in accordance with the guide for the Care and Use of Laboratory Animals published by the US National Institutes of Health.

2.4. Cell viability assay

Cell viability was evaluated by MTT assay. Briefly, RAW264.7 cells (100 μl) were plated at a density of 2 $\times$ 10^5 cells/ml in 96-well plates in a 37 °C, 5%CO$_2$ incubator. After an overnight culture period, cells were washed with DMEM and incubated with 50 μl of tylvalosin at different concentrations (0, 0.5, 1, 5, 10 μg/ml) for 1 h, followed by stimulation with 50 μl LPS (4 μg/ml). The total volume of each well was 200 μl, and the concentrations of tylvalosin and LPS were four times diluted finally. After 18 h of LPS stimulation, 20 μl of MTT solution (5 mg/ml in PBS), and 180 μl of fresh culture medium were added. After cells were incubated for 4 h at 37 °C and 5% CO$_2$, the supernatant was removed and 150 μl DMSO was added to each well to dissolve produced formazan crystals. The extinction was measured at 570 nm using a microplate reader (Thermo Scientific, USA). Cell viability was defined relative to untreated control cells [i.e., viability (% control) = 100 $\times$ (absorbance of treated sample)/(absorbance of control)].

2.5. Measurement of proinflammatory cytokines production

Tylvalosin solubilized with PBS was diluted with DMEM prior to treatment. RAW 264.7 cells were plated onto 24-well plates (10^{5}cells/well), and incubated in the presence of either LPS alone 1 μg/ml, or LPS plus tylvalosin 0.5 μg/ml, 1 μg/ml, 5 μg/ml and 10 μg/ml for 18 h. Cell-free supernatants were subsequently employed in proinflammatory cytokine assays using a ELISA kit following protocol of the manufacturer.

2.6. Measurement of nitrate/nitrite production using Griess reagent

Nitric oxide (NO) production in RAW264.7 cell culture supernatant was determined with the Griess reaction. The supernatant was collected, and mixed with equal Griess reagent (0.1% *N*-(1-naphthyl)-ethylenediamine dihydrochloride in H$_2$O and 1% sulfanilamide in 5% concentrated H$_3$PO$_4$; vol 1:1), then shaken lightly for 10 min at room temperature. At last, absorbance value (*A*) of triplicate samples was read on microplate reader using a test wavelength of 540 nm and nitrite concentration was determined using a dilution of sodium nitrite as standard.

2.7. Determination of the anti-PRRSV effect of tylvalosin

PRRSV cultures in cells treated with tylvalosin (1 μg/ml) or not were collected 20 h after viral infection. After three freeze–thaw cycles, the cultures were serially diluted 10-fold from 10^{-1} to 10^{-10}, and added to Marc-145 cells at 50–60% confluence in 96-well plates. Each dilution was added to four wells. After 5–7 days of infection, the TCID$_{50}$ was calculated by the Reed–Muench method. All experiments were done in triplicate.

2.8. Measurement of intracellular ROS

LPS-induced intracellular ROS generation was determined in RAW264.7 cells using the ROS sensitive fluorescent dye DCFH$_2$-DA. To observe intracellular ROS production through the oxidation of DCFH$_2$-DA, near confluent cells on round coverslips in 6-well plates were pretreated with tylvalosin (0.1, 0.5, 1, 5, 10 μg/ml) for 4 h and co-incubated with LPS (1 μg/ml) and DCFH$_2$-DA (10 μM) for 20 min. Cells were washed twice with PBS, and the intracellular

levels of ROS were analyzed by microscopy. DCF fluorescence intensities were determined from the same numbers of cells in randomly selected areas.

MARC-145 cells were infected with PRRSV strain Hn at MOI = 0.1 for indicated time points (12, 24, 36 and 48 h) post-infection (p.i.) in the presence of either virus alone, or virus plus tylvalosin (1 μg/ml). Cells were treated with DCFH$_2$-DA (10 μM) for 15–20 min and washed twice with PBS, and the intracellular levels of ROS were analyzed by the microscopy. DCF fluorescence intensities were determined from the same numbers of cells in randomly selected areas.

2.9. Western blot analysis

RAW 264.7 cells (4×10^5) were plated onto 6-well plates and incubated overnight, then pretreated with tylvalosin (0.5, 1, 5 and 10 μg/ml) for 1 h. After LPS (1 μg/ml) stimulation for 30 min, the cells were collected and washed twice with cold PBS. The cells were lysed in lysis buffer containing 50 mM Tris (pH 7.6), 150 mM NaCl, 5 mM EDTA (pH8.0), 0.6% NP-40, 1 mM Na$_3$VO$_4$, 20 mM β-glycerophosphate, 1 mM phenylmethylsulfonyl fluoride, 2 mM p-nitrophenyl phosphate, and 1:25 Complete Mini Protease Inhibitor cocktail (Boehringer, Mannheim, Germany) and maintained on ice for 30 min. The cell lysates were washed via dilution and centrifugal concentration. Nuclear and cytoplasmic fractions were extracted by protein extraction reagent. The protein concentrations were determined using a BCA protein assay kit (Beyotime, Haimen, Jiangsu Province, China) before storage at −80 °C. Aliquots of the lysates were separated on 10% SDS–polyacrylamide gel and transferred onto a polyvinylidene fluoride (PVDF) membrane (Millipore, Billerica, MA, USA) with a glycine transfer buffer [192 mM glycine, 25 mM Tris–HCl (pH8.8), 20% methanol (v/v)]. After blocking the nonspecific site with blocking solution (5% (wt/vol) nonfat dry milk), the membrane was incubated with specific primary antibody for 1 h at RT or overnight at 4 °C. The membrane was then incubated for an additional 60 min with a peroxidase conjugated secondary antibody at room temperature. The immunoactive proteins were detected using an enhanced chemiluminescence (ECL) Western blotting detection kit (Pierce, Rockford, IL, USA).

2.10. Mouse model

ICR mice were intragastrically administrated PBS with or without tylvalosin (25, 50 and 100 mg/kg) 2 h prior to intraperitoneal administration of LPS (15 mg/kg) and were then rested for 4 h and 24 h. A control animal was produced with the injection of PBS. The number of mice used in each treatment is ten.

At select time points after LPS administration, blood was collected for further analysis. The left lung was used to collect bronchoalveolar lavage fluid (BALF), which was lavaged four times with 1.2 ml of PBS via the intratracheal route. The BALF from each sample was centrifuged (4 °C, 3000 × g, 10 min) to pellet the cells. The total cells were pooled and resuspended in 200 μl PBS for cell counts using a hemacytometer and supernatants were stored at −80 °C for subsequent analysis of protein, MPO, and cytokine levels. Differential cell counts were determined using cytological preparations. Slides were prepared with a cytospin and were stained with Diff-Quik after which a total of 500 cells counted by microscopy. Superior lobe of right lung was used for histopathologic evaluation and PLA2 activity analysis. Inferior lobe of right lung was used to obtain lung wet-to-dry weight (W/D) ratio.

2.10.1. Lung wet-to-dry weight (W/D) ratio

In the present study, lung wet-to-dry weight ratio was calculated to assess tissue edema. Mice were euthanized at 4 or 24 h after LPS challenge. Inferior lobe of right lung was blotted dry, weighed, and then placed in an oven at 80 °C for 48 h to obtain the "dry" weight. The ratio of the wet lung to the dry lung was calculated to assess tissue edema.

2.10.2. Protein analysis

Protein concentrations in the supernatant of the BALF were quantified using BCA protein assay kit to evaluate vascular permeability in the airways.

2.10.3. Evaluation of cytokines in BALF

Levels of IL-8, IL-6, IL-1β, TNF-α and PGE2 in the cell-free BALF were evaluated using ELISA in accordance with the manufacturer's instructions.

2.10.4. Detection of nitric oxide (NO) production

The content of nitric oxide in BALF was determined according to the colorimetric method described above.

2.10.5. Measurement of MPO activity

The activity of MPO was determined in the lung tissue by a commercial kit according to the manufacturer's instruction. One hundred milligrams of the right lung tissue (n = 4) was homogenized and fluidized in extraction buffer to obtain 5% of the homogenate. The sample including 0.9 ml homogenate and 0.1 ml of reaction buffer was heated to 37 °C in a water bath for 15 min, then the enzymatic activity was determined by measuring the changes in absorbance at 460 nm using a microplate reader.

2.10.6. Measurement of MDA

MDA concentration was determined as an indicator of lipid peroxidation in the lung tissue. The tissue samples of lung were weighed and homogenized (1:10, w/v) in 0.1 mol/l phosphate buffer (pH 7.4) in an ice bath. The homogenate was centrifuged at 3000 × g for 20 min at 4 °C. Subsequently, MDA content in the supernatants was measured using a commercial kit. The protein content of the supernatant was determined by BCA protein assay kit and the concentration of MDA was expressed as nanomoles per milligram of protein.

2.10.7. Measurement of PLA2 activity

Lung tissues were sheared, and mixed with 500 μl lysis buffer (10 mM hepes, 0.34 M sucrose, pH 7.5) containing protease inhibitor cocktail (Sigma-Aldrich, St. Louis, MO, USA). Samples were homogenized with tissue homogenizers and centrifuged at 16,000 × g at 4 °C for 40 min. The supernatant was removed to a fresh tube, and a small aliquot was retained for protein assay. PLA2 activities were analyzed using the fluorescent substrate DBPC, a fluorogenic phosphatidylcholine (PC) substrate. Lung tissue homogenate (0.02 mg protein) were mixed with DBPC (0.2 μg in 200 μl of PBS). The PLA2 activities were expressed as change in fluorescence intensity per minute per milligram of protein.

2.10.8. Histological examination

4 h or 24 h after treatment, the left lungs and livers were isolated, placed into a tube containing 4% paraformaldehyde in 0.1 M PBS (pH 7.2) and incubated overnight at 4 °C. After washing three times, the tissues were processed in preparation for paraffin embedding and cut into 5-μm-thick sections. To examine the inflammatory aspects of the lung and liver, the sections were processed for hematoxylin and eosin (H&E) staining. Sections were air-dried on gelatin coated slides, immersed in hematoxylin for 5 min and checked for complete staining in tap water. Eosin staining was performed for 3 min. Sections were dehydrated through a graded series of alcohols (70–100% ethanol, 3 min each), cleared in xylene and mounted on coverslips. The stained sections

were photographed using the microscope above at an original magnification of 200×. Six sections from each sample were evaluated scored independently by two members of the laboratory trained in histological assessment and use of the scoring system. Briefly, three different lobes were examined for the following features: interstitial edema, hemorrhage, and neutrophil infiltration. Each feature could receive a score of 0 (no injury), 1 (minimal injury), 2 (moderate injury), or 3 (severe injury). This was totaled for a given lobe's score, and the three lobes averaged to generate a score for each mouse, giving a minimum score of 0 and a maximum of 9.

2.10.9. Immunohistochemistry

After deparaffinization, the sections were sequentially treated with 3% hydrogen peroxide (H_2O_2) in methanol for 30 min to quench endogenous peroxidases and rinsed thoroughly with PBS. Sections were blocked with 2.5% normal blocking serum in PBS at room temperature for 60 min to suppress any nonspecific binding of IgG, followed by incubation with mouse mAb iPLA2-VI, rabbit mAb cPLA2-IVA, rabbit mAb p-cPLA2-IVA, goat mAb sPLA2-IVE, rabbit mAb p-IκBα, mouse mAb IκBα, respectively. The samples were washed with PBS, incubated for 60 min at room temperature with secondary IgG, diluted in 2.5% normal blocking serum and then incubated for 60 min at room temperature with avidin–biotin–peroxidase complex (ABC Elite kit; Vector Laboratories, Burlingame, CA, USA). The samples were then washed with PBS and incubated for 7–10 min with 0.05% 3′3-diaminobenzidinetetrahydrochloride (DAB) (Sigma-Aldrich, St. Louis, MO, USA) and 0.003% hydrogen peroxide for 10 min in dark to assess immunoreactivity, after which the sections were counterstained with eosin and mounted. To verify the immunoreactivity specificity for iPLA2-VI, cPLA2-IVA, p-cPLA2-IVA, sPLA2-IVE, MPO, IκBα and p-IκBα, sections were also incubated with only the primary antibody (no secondary) or with only the secondary antibody (no primary). In these situations, no positive staining was found in the sections, indicating that the immunoreaction was positive in all the experiments carried out. All slides were observed with the microscope above. Immunocytochemistry photographs ($n = 6$) were assessed by densitometry. Immunoreactivity was analyzed through image pro plus software (Media Cybernetic, Silver Spring, USA) on a personal computer. For every section, the integral optical density (IOD) of every visual field was calculated.

2.11. Pig study

In total, 20 pigs were ear-tagged and randomly allocated to 1, 2, 3 and 4 ($n = 5$) group. Pigs belonging to the medication groups (1 and 2) received a feed containing 75 p.p.m. tylvalosin for 28 days. At 28 day post-medication, the groups (1, 2 and 3) of pigs were infected with 2 ml pernostril of PRRSV strain Hn at a $TCID_{50}$ of $10^{4.5}$ ml^{-1}. The four group of pigs received uninfected culture supernatant in a similar manner and served as nonmedicated and nonchallenged control pigs. After challenge, pigs in group 1 continued to receive tylvalosin medicated feed for another 21 days. Clinical signs and rectal temperatures were recorded daily and blood samples were taken on days 3, 5, 7, 10, 14, 18 and 21 post-inoculation (p.i.), and sera was aliquoted and stored at −80 °C for later analysis. Animals were also weighed on a weekly basis. Pigs were necropsied at the end of the experiment or when died or euthanized because of severe illness.

2.11.1. Pathological examination

Complete necropsies were performed on all pigs, and all organs were examined with emphasis on the respiratory tract. Lungs were given a score to estimate the percentage of the lung surface affected, using a scoring system previously reported to evaluate gross lung lesions [21].

2.11.2. Viremia detection by RT-PCR

RT-PCR was performed on sera collected on day 3, 5, 7, 10, 14, 18 and 21 p.i. The extraction of viral RNA was performed using the QIAamp Viral RNA Mini-Kit (Qiagen, Valencia, CA, USA) as described in the kit instructions. The RT-PCR assay kit for PRRSV detection was purchased from Takara (Dalian, Liaoning province, China) and used according to kit instructions.

2.12. Statistical analysis

Quantitative data are given as mean values ± SD or as indicated. For analysis of differences between the groups, ANOVA followed by the appropriate post hoc test for individual comparisons between the groups was performed. All tests were two-tailed. $P < 0.05$ was considered statistically significant.

3. Results

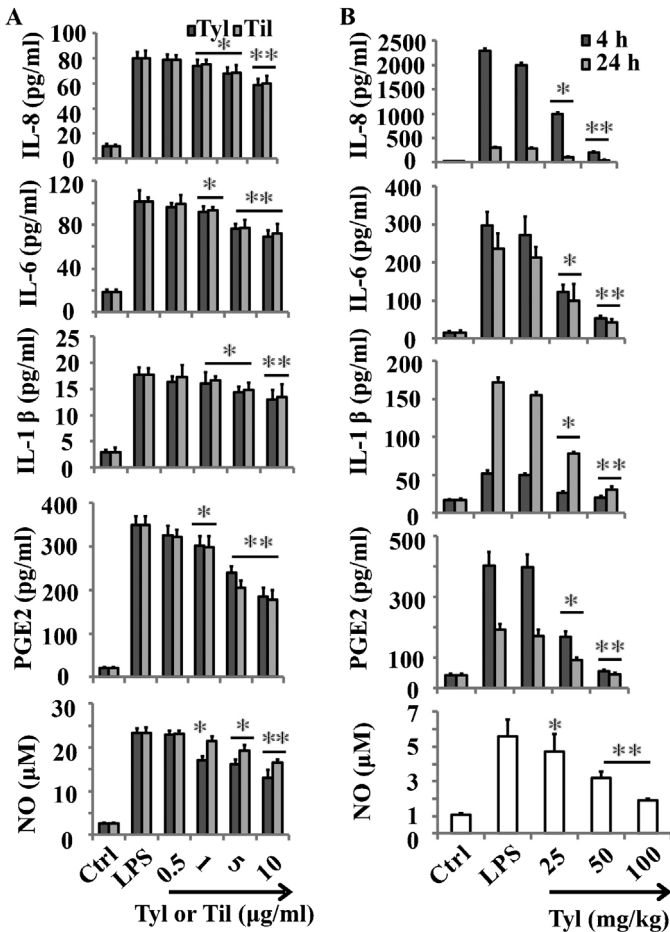### 3.1. Tylvalosin suppresses LPS-induced proinflammatory cytokines production

The levels of IL-8, IL-6, IL-1β, PGE2, and TNF-α in the culture supernatants were measured using ELISA kits. Treatment of RAW 264.7 cells with LPS alone resulted in significant increase in cytokine production compared to the drug groups (Figs. 2 and 3C). However, the levels of TNF-α, PGE2, IL-8 IL-6 and IL-1β in the supernatants of LPS stimulated cells pretreated with 1, 5 and 10 μg/ml tylvalosin and tilmicosin were reduced significantly compared to the LPS group in a dose dependent manner (* $P < 0.05$, ** $P < 0.01$) (Figs. 2 and 3C). There is no significant difference between tylvalosin and tilmicosin. In addition, the MTT result showed that cell viabilities were not affected by the tylvalosin at the concentrations used (0.5, 1, 5 and 10 μg/ml) (data not shown). Thus, the effects of tylvalosin on RAW264.7 cells did not attribute to cytotoxic effects.

To determine the levels of cytokines in BALF, BALF was harvested 4 h and 24 h after LPS challenge. IL-8, IL-6, IL-1β, PGE2, and TNF-α levels were measured by ELISA. Proinflammatory cytokines levels in the BALF of mice treated with tylvalosin (50 and 100 mg/kg, i.g.) were significantly increased compared to those in LPS group (* $P < 0.05$, ** $P < 0.01$) (Figs. 2 and 3D).

Lung tissue sections from LPS-treated mice demonstrate strong positive staining for TNF-α (Fig. 3A and B) mainly localized in the epithelial bronchial cells (see arrows Fig. 3(a1)), in inflammatory cells in subbronchial epithelial (see arrows Fig. 3A(a2)) and in lymphocytes (see arrows Fig. 3(a3)). In LPS treated mice, which received tylvalosin treatment (50 and 100 mg/kg, i.g.), the staining for TNF-α was visibly and significantly reduced in comparison with the vehicle-treated mice (Fig. 3B and D). No positive staining for TNF-α was found in the lung tissues from sham-treated mice (Fig. 3A).

3.2. Tylvalosin suppresses proinflammatory mediator level

LPS administration also significantly enhanced the production of NO, as indicated by an increase in nitrite/nitrate (Fig. 2A) in the stimulated RAW264.7 cells, compared to the Ctrl. When cells stimulated with LPS in the presence of tylvalosin or tilmicosin (0.5, 1, 5 and 10 μg/ml), a concentration-dependent inhibition of NO generation was observed (Fig. 2B). Both of them at higher concentration (5 and 10 μg/ml) significantly inhibited NO release. Specially, tylvalosin showed higher inhibition effect of NO release.

Fig. 2. Tylvalosin suppresses LPS-induced proinflammatory cytokines production. (A) Effects of different concentrations of tylvalosin and tilmicosin on LPS-induced IL-8, IL-6, IL-1β, PGE2 and NO in LPS stimulated RAW 264.7 cells. The cells were treated with LPS alone or LPS plus different concentrations (0.5, 1, 5 and 10 μg/ml) of tylvalosin and tilmicosin for 18 h. (B) Effects of tylvalosin on the production of proinflammatory cytokines IL-8, IL-6, IL-1β, PGE2 and NO in the BALF. Mice were given tylvalosin (25, 50 and 100 mg/kg, i.g.) 2 h prior to administration of LPS. BALF was collected at 4 h and 24 h following LPS challenge to analyze the proinflammatory cytokines. The values represent mean ± SD of three independent experiments and differences between mean values were assessed by Student's t-test. $^*P < 0.05$ vs LPS, $^{**}P < 0.01$ vs LPS.

As shown in Fig. 2B, LPS i.p. injection significantly increased the levels of NO ($^{**}P < 0.01$) compared to Ctrl. Compared with LPS group, different doses of tylvalosin decreased the production of NO in BALF ($^*P < 0.05$ for 25 and 50 mg/kg, $^{**}P < 0.01$ for 100 mg/kg).

3.3. Tylvalosin attenuates oxidative stress

It has been shown that antioxidants can inhibit the NF-κB activation signaling pathway and suppress inflammation-associated gene expression in macrophages stimulated with LPS by decreasing the intracellular ROS level [22]. We tested whether tylvalosin inhibits the intracellular ROS generation in RAW264.7 cells stimulated with LPS. Tylvalosin treatment strongly inhibited the LPS-mediated increase in intracellular ROS level in a dose dependent manner (Fig. 4A and C). Tylvalosin alone had no effect on ROS production (data not shown).

The production of ROS and the subsequent oxidative damage to cells and tissues, are recognized as key contributors to viral pathogenesis. ROS-mediated oxidative stress could also contribute to PRRSV-induced apoptosis. In the current study, continuous up-regulated generation of ROS was observed from 12 h p.i. to 24 h p.i.

(Fig. 4B and D), and then ROS induced by PRRSV declined from 24 h p.i. to 48 h p.i. gradually. Tylvalosin treatment significantly inhibited the PRRSV-mediated increase in intracellular ROS level at 24 h p.i. and 36 h p.i. (Fig. 4B and D).

Lung MDA levels, an indicator of lipid peroxidation, increased markedly in the LPS group compared with the Ctrl group (Fig. 4E), whereas the increase was significantly attenuated in the tylvalosin treatment (50 and 100 mg/kg, i.g.) group, as shown in Fig. 4E.

3.4. Tylvalosin ameliorates LPS-induced acute tissues injury and inflammation response

To assess local injury response to LPS, detailed lung and liver histological examinations were performed. As early as 4 h after LPS administration, marked differences in lung and liver injury were observed between Ctrl and LPS mice. As shown in Fig. 5A–D, perivascular exudates, thickened alveolar septa, hemorrhage, airspace edema and hepatocyte degeneration, apoptosis and necrosis were exhibited in mice treated with LPS (i.p., 15 mg/kg), but were noticeably attenuated in tylvalosin treatment ($^*P < 0.05$ for 50 mg/kg tylvalosin; $^{**}P < 0.01$ for 100 mg/kg tylvalosin) mice at both 4 and 24 h (Fig. 5E). Consistent with this injury pattern, BALF protein concentration (Fig. 5F) and lung wet:dry ratios (Fig. 5G) were increased in LPS treatment mice. However, treatment with tylvalosin (50 mg/kg and 100 mg/kg, i.g.) markedly decreased lung W/D ratio ($^*P < 0.05$ or $^{**}P < 0.001$) and total protein concentration ($^{**}P < 0.01$) in BALF of mice. Taken together, these findings indicate tylvalosin attenuates both the local and systemic response to i.p. LPS.

3.5. Tylvalosin suppresses LPS-induced inflammatory cells recruitment and activation

4 h and 24 h after challenge with LPS, the inflammatory cell levels (i.e., total cells, neutrophils, macrophages, lymphocytes and eosinophils) in the BALF were significantly elevated in LPS-challenged mice vs Ctrl mice (Fig. 6A–C). However, tylvalosin administration (25, 50 and 100 mg/kg, i.g.) ($^*P < 0.05$ for 50 mg/kg, $^{**}P < 0.01$ for 100 mg/kg) decreased the total cell number and the number of infiltrating neutrophils and macrophages in a dose-dependent manner (Fig. 6A–C), as compared with the LPS-challenged mice.

MPO activity is another measure of lung parenchymal phagocyte infiltration. LPS challenge resulted in significant increases in lung MPO activity compared with the Ctrl group ($P < 0.01$). Tylvalosin (50 and 100 mg/kg, i.g.) 2 h before LPS exposure significantly reduced MPO activity compared with the LPS group ($^*P < 0.05$, $^{**}P < 0.01$, Fig. 6D). This result was consisted with the data that total lavage cell counts and the percentage of lympocytes and neutrophils in the BALF were reduced in LPS-treated mice that received 50 and 100 mg/kg tylvalosin compared with the group treated with LPS alone (Fig. 6A–C). Our MPO immunostaining results also supported the above data (Fig. 6E).

3.6. Tylvalosin inhibits PLA2 activity and activation

Along with these histopathological changes above, the IHC revealed the inhibitory effects of tylvalosin on PLA2 activity and activation in the lungs. The DAB staining of cPLA2-IVA, p-cPLA2-IVA and sPLA2-IVE in the lung demonstrated the diminished expression of PLA2 by tylvalosin (Fig. 7). Note the deep staining of cPLA2-IVA, p-cPLA2-IVA and sPLA2-IVE in the epithelial bronchial cells (see arrows (a1)), in inflammatory cells in subbronchial epithelial (see arrows, (a2)), and in leukocytes (a3) with DAB in the LPS-treated mice. Interestingly, this phenomenon was attenuated by tylvalosin (50 and 100 mg/kg, i.g.) significantly. Higher levels of
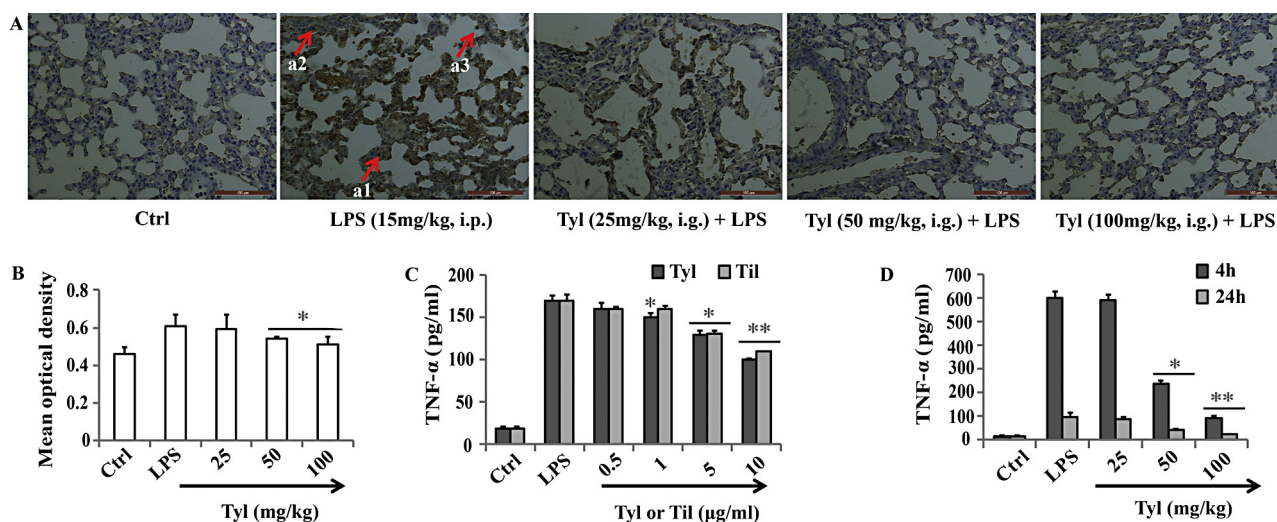
Fig. 3. Tylvalosin suppresses TNF-α level. (A) Immunohistochemical localization of TNF-α in the lung. Immunohistochemical analyses for TNF-α show positive staining for TNF-α mainly localized in the epithelial bronchial cells (see arrows a1), in inflammatory cells in subbronchial epithelial (see arrows, a2), and in lymphocytes (a3). Figure is representative of at least three experiments performed on different experimental days. Original magnification 200×. (B) Quantitative immunohistochemical expression of TNF-α expression in lungs. The immunohistochemical images were analyzed quantitatively using Image Pro-Plus v6.0. Density means are expressed as mean ± SD. Quantitative analysis showed significantly decreased expression of TNF-α in lungs from mice treated with tylvalosin (50 and 100 mg/kg, i.g.). (C) Effects of different concentrations of tylvalosin and tilmicosin on LPS-induced TNF-α in LPS stimulated RAW 264.7 cells. The cells were treated with LPS alone or LPS plus different concentrations (0.5, 1, 5 and 10 μg/ml) of tylvalosin and tilmicosin for 18 h. (D) Effects of tylvalosin on the production of TNF-α in the BALF. Mice were given tylvalosin (25, 50 and 100 mg/kg, i.g.) 2 h prior to administration of LPS. BALF was collected at 4 h and 24 h following LPS challenge to analyze the proinflammatory cytokines. The values represent mean ± SD of three independent experiments and differences between mean values were assessed by Student's t-test. * $P < 0.05$ vs LPS, ** $P < 0.01$ vs LPS.

PLA2 activity were found in homogenates of lungs from LPS-treated mice compared with Ctrl mice (Fig. 8). This activity was significantly reduced in mice with tylvalosin (* $P < 0.05$ for 50 mg/kg, ** $P < 0.01$ for 100 mg/kg, i.g.).

3.7. Tylvalosin attenuates PRRSV-induced clinical disease and improve growth

The cytotoxic effect of tylvalosin on Marc-145 cells evaluated using the MTT assay above. Results showed that tylvalosin displayed no cytotoxic effect at the concentration less than 100 μg/ml (data not shown). The inhibitory effect of tylvalosin on PRRSV isolation infections was investigated by TCID$_{50}$ and virus yield reduction assays. Results showed that tylvalosin has the ability to inhibit different PRRSV isolations infection in Marc-145 cells (Fig. 9A). The virus yield reduction in TCID$_{50}$ increased from 0.55 log to 0.9 log at the concentration of 1 μg/ml for tylvalosin (Fig. 9A). This result indicated that all of the PRRSV isolations were sensitive to tylvalosin.

After challenge, all the pigs in the group 3 showed clinical signs, including reddened skin, inappetence, lethargy, rough hair coats, dyspnoea, periocular edema, eyelid oedema and slightly diarrhea (data not shown). Similar clinical signs of low intensity were observed in the groups 1 and 2. All animals had rectal temperatures taken daily after challenge. PRRSV infected animals had mean temperatures in group 3 which increased above other groups between 2 and 9 days p.i. and exceeded 40 °C, temperature considered to be hyperthermia, at 3, 4, 5, 6, 7, 8 and 9 days p.i. These temperatures were significantly higher than pigs in group B at 3 and between 3 and 6 days p.i. The pigs in group 1 showed slight fever (40.0–40.2 °C) and a little fluctuation of rectal temperatures at 14 days p.i. (Fig. 9B). Mean temperatures of group 4 remained below 40 °C during the experiment.

Viraemia was determined by RT-PCR on serum samples. All animals were negative for viral RNA on 0 dpi and the animals in groups 1 and 2 remained negative throughout the study. Results are encouraging enough to merit further work to study this phenomenon. Viral RNA was detected in all virus-infected group 3 on 3 days p.i., four animals at 7 days p.i. and 14 days p.i.

To assess the gross clinical effects of tylvalosin medication on swine, all animals were weighed at each time point. From this data, average daily weight gain (ADWG) was derived for −28 days p.i. (before inoculation) and 21 days p.i. (Fig. 9C). Before challenge (−28 dpi), there is slight weight increase for pigs in the group 1 and 2 although no significant ($P > 0.05$). After challenge, group 3 showed significantly reduced ADWG compared to other animals in group 1, 2 and 4. In addition, group 1 had a statistically significant higher ADWG than group 2, signifying that tylvalosin significantly reduced animal growth because of challenge.

At post-mortem, the lungs were examined for gross pathology and were given a score dependent on the percentage of the lung surface to be affected by gross lesions, with a maximum of 100 points. Group 3 had the average highest score of around 52% of the surface of the lung affected by lesions (Fig. 9D). There was the lowest mean score being seen in the 1 group followed by 2 around 37% of the surface of the lung affected by lesions. The nonmedicated and nonchallenged animals in group 4 euthanized showed no significant pathology.

3.8. Tylvalosin suppresses LPS-induced NF-κB pathway activation

Phosphorylation of IκB and the p65 subunit of NF-κB is an important event in translocation and the transcriptional activity of NF-κB. In unstimulated cells, NF-κB is localized to the cytosol due to its binding with IκB. Once activated by LPS, IκB is phosphorylated by IκB kinase and degraded, and then the released NF-κB is translocated into the nucleus [23]. Therefore, the activation of NF-κB was assessed in RAW264.7 cells by measuring the degree of phosphorylation of IκBα protein and NF-κB p65 translocation. Treatment with LPS resulted in the degradation of IκBα and this degradation was significantly blocked by tylvalosin (Fig. 10A and B). To determine whether this IκBα degradation was related to IκBα phosphorylation, we examined the effect of tylvalosin on LPS-induced p-IκBα by western blot. The results showed that the
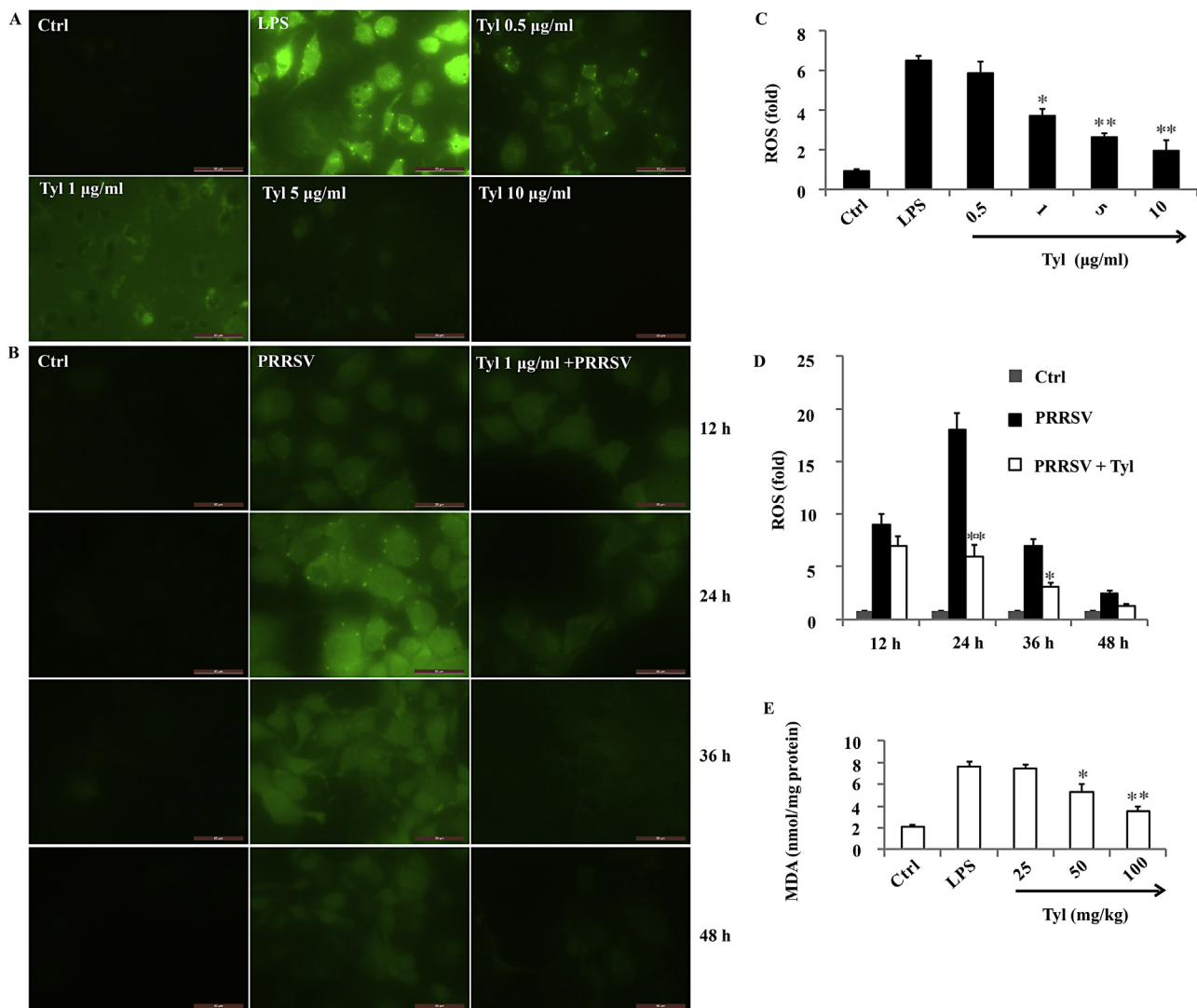
Fig. 4. Tylvalosin attenuates oxidative stress. (A) Representative photos from RAW264.7 cells treated with tylvalosin at indicated concentration and co-incubated with LPS (1 μg/ml) for 18 h. Cells were washed twice with PBS, and the intracellular levels of ROS were analyzed by fluorescence microscopy. (B) Representative photos from Marc-145 cells treated with tylvalosin (1 μg/ml) and co-incubated with PRRSV Jx (MOI =1) for 12, 24, 36 and 48 h, respectively. Cells were washed twice with PBS, and the intracellular levels of ROS were analyzed by fluorescence microscopy. (C) Effects of tylvalosin on the LPS-induced ROS generation in RAW264.7 cells. RAW264.7 cells (2×10^5 cells/well in 24-well culture plates; $n = 6$) were treated with tylvalosin at indicated concentration and co-incubated with LPS (1 μg/ml) for 18 h. DCFH2-DA (10 μM) was used to determine the generation of intracellular ROS. DCF fluorescence intensities were determined from the same numbers of cells in randomly selected areas. (D) Effects of tylvalosin on the LPS-induced ROS generation in RAW264.7 cells. RAW264.7 cells (2×10^5 cells/well in 24-well culture plates; $n = 6$) were treated with LPS (1 μg/ml) for 18 h with tylvalosin at indicated concentration and co-incubated with LPS (1 μg/ml). DCFH2-DA (10 μM) was used to determine the generation of intracellular ROS. DCF fluorescence intensities were determined from the same numbers of cells in randomly selected areas. (E) Effects of tylvalosin on the lung MDA levels. MDA level was significantly increased in LPS-treated mice compared with ctrl mice. This increase in MDA level was significantly reduced by posttreatment with tylvalosin (50 and 100 mg/kg, i.g.). The data are mean ± SD ($n = 6$). * $P < 0.05$ vs LPS group; ** $P < 0.01$ vs LPS group. Original magnification 400×.

phosphorylation of IκBα in RAW264.7 cells increased after LPS administration but was significantly inhibited by tylvalosin in a concentration dependent manner (Fig. 10A and B). To gain further insight into the mechanism of tylvalosin-mediated regulation of NF-κB, we examined the effect of tylvalosin on NF-κB p65 nuclear translocation. As shown in Fig. 10C and D, LPS-treated cells showed a notably increased nuclear protein level and a decreased cytoplasmic protein level, compared to PBS-treated RAW264.7 cells, tylvalosin treatment significantly attenuated these alterations in a dose-dependent manner (* $P < 0.05$, ** $P < 0.01$).

To determine the effects of tylvalosin treatment on in vivo activation of the classical NF-κB pathway, lung tissue sections of mice were analyzed for p-IκBα and IκBα by IHC. As shown in Fig. 11A, IHC analysis revealed p-IκBα staining intensity to be higher in the LPS group when compared with the Ctrl animals, predominantly localized within the cytosol. Treatment with

tylvalosin reduced the number of p-IκBα staining intensity compared with the LPS group (Fig. 11A), and this was the reverse case with IκBα (Fig. 11B). Quantitative analysis showed significantly decreased expression of p-IκBα and increased expression of IκBα in lungs after mice treated with tylvalosin (50 and 100 mg/kg, i.g.) (Fig. 11C and D).

4. Discussion

Tylvalosin is a new broad-spectrum antibiotic, belonging to third-generation macrolides with its usefulness. This study was to evaluate whether tylvalosin exerts anti-inflammatory effects in LPS-stimulated RAW 264.7 cells and animal models of ALI. The collective results of this investigation demonstrate that tylvalosin inhibits inflammation by reducing the expressions of pro-inflammatory mediators normally regulated by the NF-κB
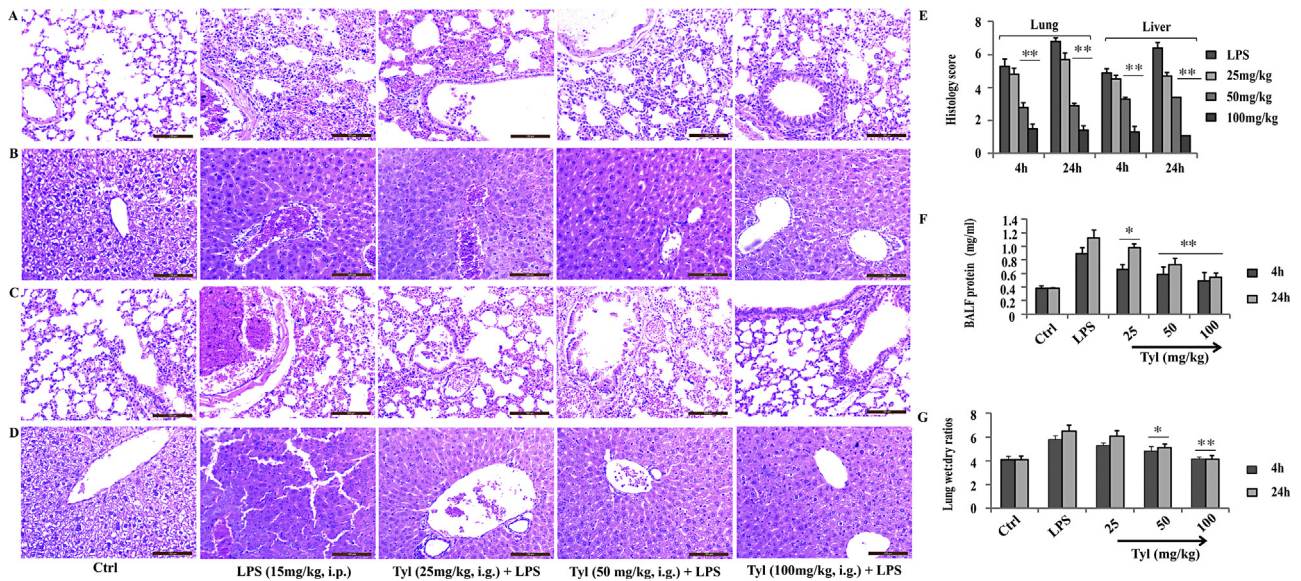
Fig. 5. Tylvalosin ameliorates LPS-induced acute tissues injury and inflammation response in mice 4 h and 24 h after i.p. PBS or LPS. ((A) and (B)) Lung and liver histological examination 4 h after i.p. PBS or LPS demonstrated increased perivascular exudates (arrow), thickened alveolar septa (asterisk), airspace edema, apoptosis and necrosis in LPS treated mice when compared with tissues of tylvalosin ($P < 0.01$ for 50 and 100 mg/kg) treated mice. ((C) and (D)) Twenty-four hours after LPS injection, LPS mice continued to have more severe lung and liver injury than tylvalosin ([**] $P < 0.01$ for 50 and 100 mg/kg) treated mice. Original magnification 200×. (E) LPS treatment mice had more severe lung and liver injury histological scores at both 4 and 24 h, based on hemorrhage, interstitial edema, inflammatory cells infiltration and hepatocyte degeneration, apoptosis and necrosis. Total BALF protein concentration (F) and wet:dry ratio (G) were increased in LPS mice after i.p. LPS when compared with ctrl mice and tylvalosin treatment mice ($n = 10$ each group, replicated 3 times for histology, wet:dry, BALF protein, [*] $P < 0.05$, [**] $P < 0.01$; histological scores were from three mice per group, three lobes examined per mouse).

pathway, as well as downregulating of PLA2 and ROS. Our results indicated that tylvalosin might be a potential new therapeutic agent in the prevention and treatment of inflammatory diseases.

To assess the pharmacological and biological effects of tylvalosin on the production of proinflammatory cytokines in LPS-stimulated RAW 264.7 macrophages, the roles of tylvalosin in suppression of production of proinflammatory cytokines and

blockage of NF-κB signaling pathways were examined. The results demonstrated that tylvalosin inhibited secretion of TNF-α, IL-6, IL-1β, IL-8, PGE2 and NO in a dose dependent manner (Figs. 2 and 3). Tylvalosin and tilmicosin are semi-synthesized compounds derived from tylosin, belonging to 16-membered macrolides. Consistent with the previous study [24], the present study also shown that tilmicosin significantly decreased the production of
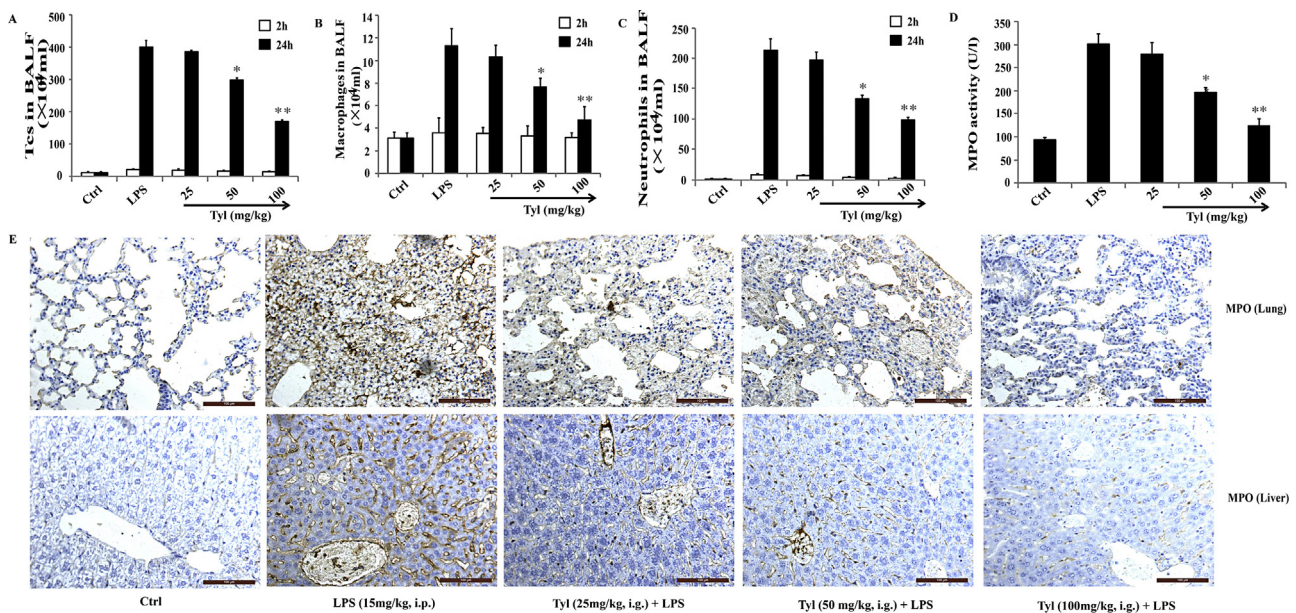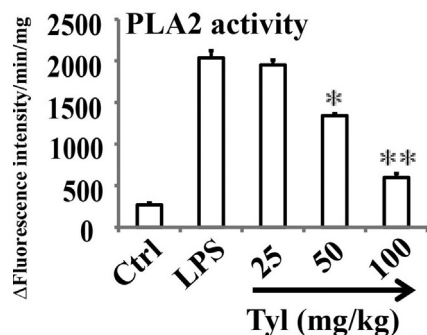

Fig. 6. Tylvalosin suppresses LPS-induced inflammatory cells recruitment and activation. BALF was collected at 4 h and/or 24 h following LPS challenge to measure the number of total cells (Tcs) (A), macrophages (B), and neutrophils (C) based on the differential cell identification. MPO activity (D) in BALF at 24 h was determined with a kit by measurement of the H_2O_2-dependent oxidation of an odianisidine solution. The values presented are the mean ± SD ($n = 6$ in each group). [*] $P < 0.05$, [**] $P < 0.01$ vs LPS group. Superior lobe of right lung and liver were processed at 24 h following LPS challenge to analyze MPO expression with immunohistochemistry. Representative immunostaining (E) for myeloperoxidase (MPO) on lung and liver sections were presented. Alveolar epithelial cells (arrows) in close proximity to degranulated neutrophils stained positive for MPO. Endothelial cells (arrowheads) near intravascular undegranulated neutrophils stained negative for MPO. Scale bars = 100 μm. Figure is representative of at least three experiments performed on different experimental days. Original magnification 200×.
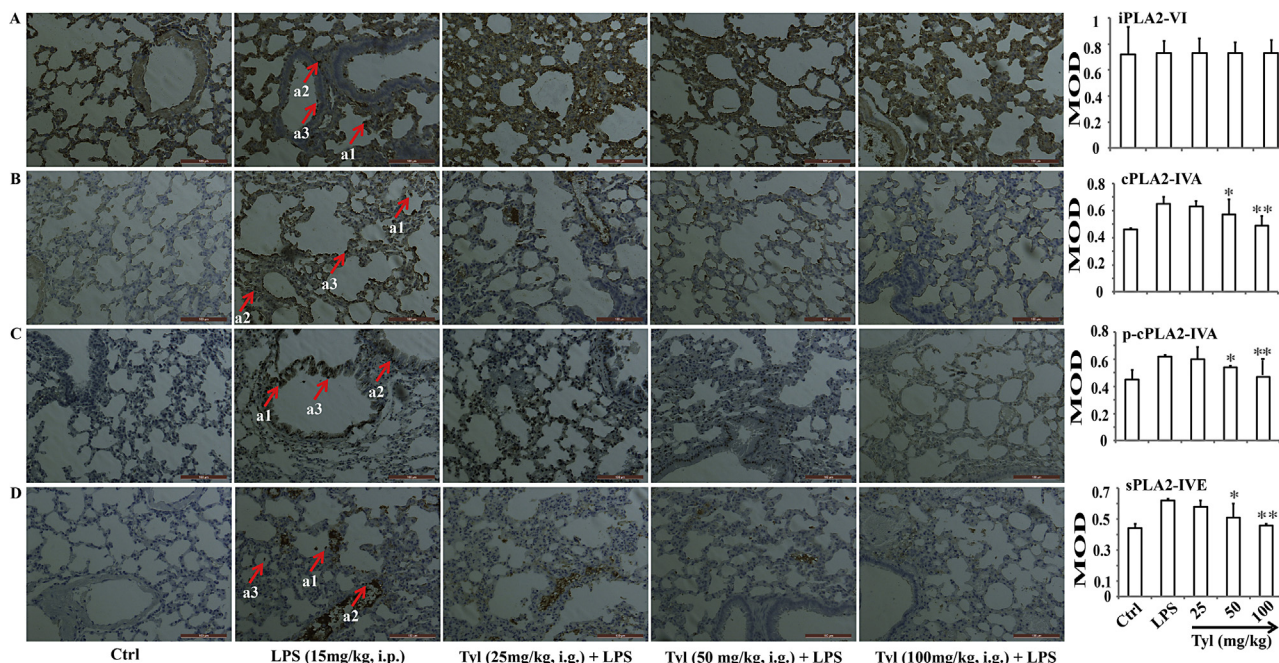
Fig. 7. Tylvalosin inhibits PLA2 expression and activation. (A) iPLA2 VI, (B) cPLA2-IVA, (C) p-cPLA2-IVA and (D) sPLA2-IVE were analyzed by immunohistochemistry in sections of lungs from ctrl, LPS and LPS + tylvalosin (25, 50 and 100 mg/kg, i.g.) treatment mice. Representative photomicrographs of staining are shown with arrows. Immunohistochemical analyses for PLA2 show positive staining for PLA2 mainly localized in the epithelial bronchial cells (see arrows a1), in inflammatory cells in subbronchial epithelial (see arrows, a2), and in leukocytes (a3). Score analysis of positive cells, performed on Ctrl, LPS and LPS + tylvalosin (25, 50 and 100 mg/kg, i.g.) treatment mice. Strong immunostaining was observed in the epithelial bronchial cells (see arrows a1), in inflammatory cells in subbronchial epithelial (see arrows, a2), and in leukocytes (a3) from LPS-treated mice. The immunohistochemical images were analyzed quantitatively using Image Pro-Plus v6.0. Mean optical density (MOD) are expressed as mean ± SD. Original magnification 200×.

TNF-α, IL-6, IL-1β, PGE2, and NO. Taken together with our findings reported here, this suggests that like the 14- and 15-member macrolides, the 16-member macrolides also have anti-inflammatory activity apart from their antibacterial activity. As to the production of TNF-α, IL-6, IL-1β, IL-8 and PGE2, there is no difference between tylvalosin and tilmicosin treatment. This result indicated that the anti-inflammatory activity depended on their parent ring (lactone ring) (Fig. 1) and seemed to have nothing to do with their side chain modification. However, tylvalosin even in the lower concentration showed higher inhibition effect of NO release comparable to that of tilmicosin. This difference could be attributed to tylvalosin side chain modification with 3-O-acetyl-4′-O-isovaleryl. Furthermore, tylvalosin exhibits rapid entry and accumulation than tilmicosin [19]. Tylvalosin is rapidly metabolized with 50% being metabolized within 30 min. The main metabolite is 3-O-acetyltylosin, which possesses equivalent activity to the parent compound. The information gained from
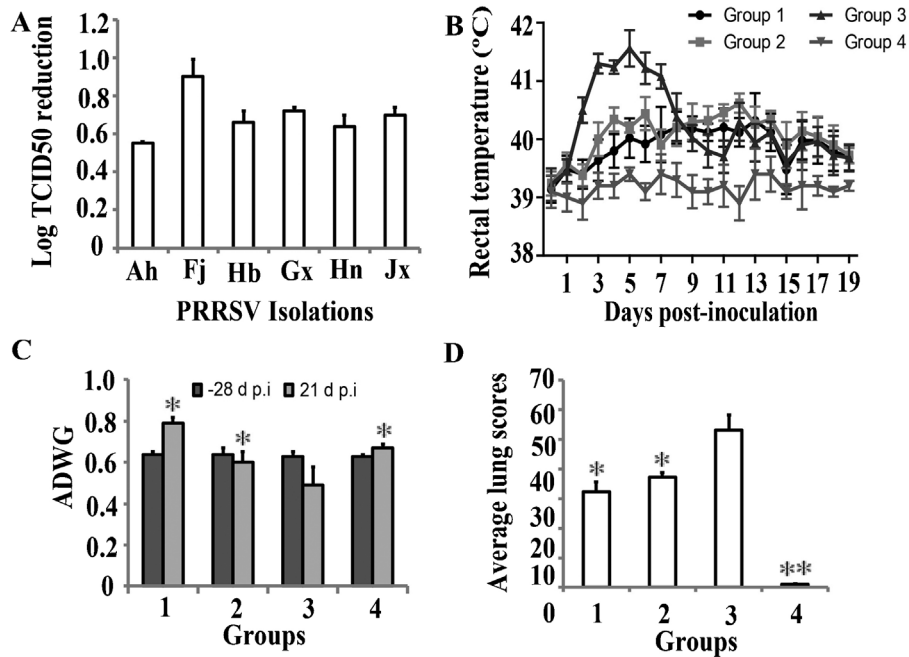
this study could be very useful for the further design and development of novel macrolides.

In agreement with the in vitro results, we found that tylvalosin played a potent anti-inflammatory role in LPS-induced ALI in mice. Tylvalosin significantly attenuated LPS stimulated pulmonary morphological changes such as lung edema, alveolar hemorrhage and inflammatory cells infiltration (Fig. 5). Apart from lung, exposure of humans and animals to excessive amounts of LPS also causes liver injury, and kupffer cells mediate LPS-induced inflammatory responses in the liver. The present study suggested that tylvalosin also significantly attenuated LPS stimulated liver morphological changes such as hepatocyte degeneration, apoptosis and necrosis. The data above indicated that tylvalosin could attenuate systemic inflammation induced by LPS.

To quantify the magnitude of pulmonary edema, we evaluated the W/D ratio of the lung. Our experiments shown that tylvalosin may significantly inhibit edema of the lung, as indicated by a W/D ratio in the tylvalosin group that was significantly lower than the LPS group (Fig. 5G). As another index of ALI by LPS, we measured total protein concentration in the BALF (Fig. 5F), which indicates epithelial permeability and pulmonary edema. As expected, LPS injection was found to cause a significant increase in BALF protein concentration. LPS-induced increases in total protein in the BALF were inhibited by tylvalosin.

Inflammatory cells count in the BALF reflects extravasation. The predominant inflammatory cells are neutrophils, which play an important role in the development of most cases of ALI [3], and may represent a potential target for therapy. Consequently, we address the effect of tylvalosin treatment on ALI and on neutrophil effector functions. In addition to the involvement of the neutrophils, macrophages are known to play a crucial role in LPS-induced ALI [25]. In this study, mice exposed to LPS exhibited a massive recruitment of inflammatory cells, including neutrophils and macrophages (Fig. 6). In contrast, pre-treatment with tylvalosin inhibited the increase in the number of total cells,

Fig. 8. Tylvalosin inhibits PLA2 activity. PLA2 activity was measured in homogenates of lungs from ctrl mice and LPS-treated mice using the DBPC-based fluorometric method. Data are means ± SD from five analyses. Omission of the primary antibody or incubation with an irrelevant antibody showed no signal (not shown). * P < 0.05; ** P < 0.01 vs LPS.

Fig. 9. Tylvalosin attenuates PRRSV-induced clinical disease and improve growth. (A) The antiviral effect of tylvalosin on PRRSV isolations infection. Marc-145 cells were treated with 1 μg/ml tylvalosin for 4 h, and then infected with PRRSV isolations. At 20 h post-infection, virus was harvested and titers were determined. The values of Log TCID50 reduction shown here are the mean ± SD of three independent experiments. (B) Rectal temperatures were monitored daily for pigs in the groups 1, 2, 3 and 4 (n = 5). Temperature above 40 °C was considered febrile. Data represented as mean ± SD. (C) Growth effects of tylvalosin on swine. All experimental pigs were weighed at Days 1, 28 and end of study. The average daily weight gain (ADWG) from five pigs in each group was calculated at period of 1 to 28 and 28–49 dpi. Data represented as mean ± SD. (D) Tylvalosin medication on the effect of lung lesion scores. Animals were sacrificed at 21 dpi when lungs were scored for gross pathology. Gross pathology data represented mean ± SD. Significance is indicated by: * P < 0.05, ** P < 0.01.

neutrophils, and macrophages in the BALF. In addition, the lung histological examination (Fig. 5) above also supported this finding. The infiltration of proinflammatory cells, hemorrhage, formation of hyaline membranes, alveolar edema, and airway epithelial necrosis were found to be common and prominent in the LPS group but rare in the tylvalosin (50 and 100 mg/kg, i.g.) treatment groups. These results suggested that the protective effect of tylvalosin on ALI was related to an attenuation of inflammatory cell sequestration and migration into the lung tissue. Neutrophil recruitment in

the lung involves in a cascade-like fashion of activation, intravascular accumulation and transendothelial and transepithelial migration, where different adhesion molecules and chemokines are involved in neutrophil recruitment. Therefore, the detailed mechanism for the tylvalosin inhibition activity on neutrophil recruitment and activation needs further study.

There exists the increased MPO activity with the infiltration of neutrophils in the lung during ALI. So, MPO activity, a marker of neutrophil influx into tissue and directly proportional to the
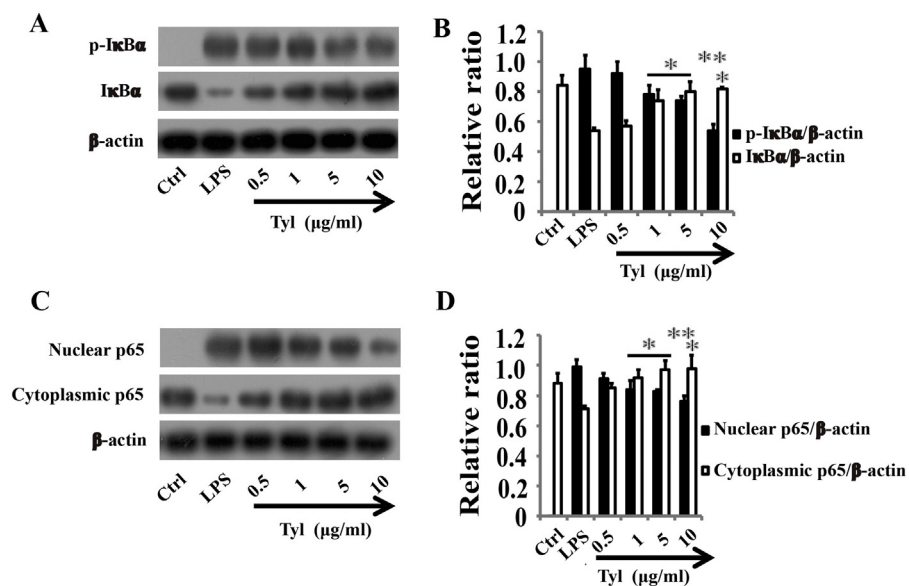
Fig. 10. Tylvalosin suppresses LPS-induced IκBα phosphorylation and degradation, and NF-κB p65 translocation in RAW264.7 cells. RAW 264.7 cells were treated in the presence of either LPS (1 μg/ml) alone, or LPS plus tylvalosin (0.5, 1, 5 and 10 μg/ml). Protein samples were analyzed by western blot with special antibodies. Quantification of protein expression was normalized to β-actin using NIH ImageJ v1.46. The data are representative of three independent experiments and expressed as mean ± SD. * P < 0.05 vs LPS, ** P < 0.01 vs LPS.
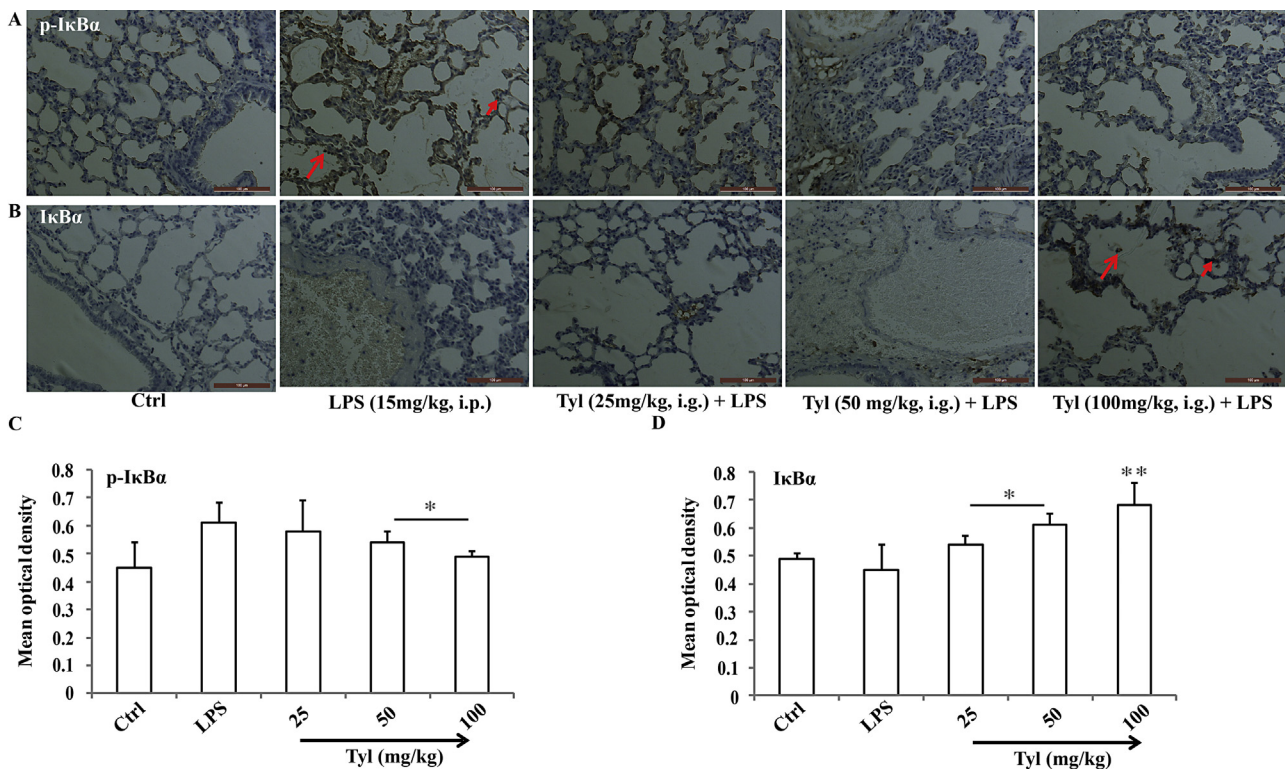
Fig. 11. Tylvalosin suppresses LPS-induced IκBα phosphorylation and degradation in the lung tissues. ((A) and (B)) Representative immunohistochemistry for p-IκBα and IκBα of lung tissue sections from normal control, LPS and LPS + tylvalosin (25, 50, 100 mg/kg). Dark brown staining indicates p-IκBα and IκBα, blue/purple staining indicates cell nuclei. Short arrows point out alveolar epithelial type II cells, alveolar macrophages are designated by the longer arrow. The immunohistochemical images were analyzed quantitatively using Image Pro-Plus v6.0. Density means are expressed as mean ± SD. Quantitative analysis showed significantly decreased expression of p-IκBα and increased expression of IκBα in lungs after mice treated with tylvalosin (50 and 100 mg/kg, i.g.). The level of significance was set at * $P < 0.05$, ** $P < 0.01$. Original magnification: 200×.

number of neutrophils in the tissue, was studied. Our present data illustrated increased MPO activity in the lung tissue in LPS-induced ALI model, which was consistent with the MPO immunostaining results and the histopathological changes of leukocyte infiltration, while such increase was significantly reduced by two doses (50 and 100 mg/kg) of tylvalosin (Fig. 6D and E). In this study, we demonstrated that pretreatment with tylvalosin significantly improved ALI in mice, which was related to attenuation of inflammatory cells sequestration and migration into the lung tissue. In addition, significant reduction of neutrophils in BALF and lung tissue infiltration were followed by PLA2 activity decrease discussed below. These results suggested that the attenuation of LPS-induced ALI by tylvalosin might be related with the PLA2s modulation.

The antioxidant strategies regulating the intracellular levels ROS for attenuation of lung inflammatory injury have been extensively investigated [26]. Also, the results from current study showed that tylvalosin suppressed the LPS-induced ROS production in RAW264.7 cells, the PRRSV-induce ROS level in Marc-145 cells and lung MDA production in vivo (Fig. 4). Our finding provided an evidence that the anti-inflammatory effect of tylvalosin was linked to its ability to inhibit ROS production and oxidative stress.

The increased levels of proinflammatory cytokines in BALF are noted during ALI/ARDS, and the persistent elevation of these mediators may induce, enlarge and facilitate an entire or focal inflammatory reaction with a worse outcome. In line with these concepts, we found that mice challenged with LPS expressed very large amounts of these proinflammatory cytokines in the BALF compared with the negative control group (Figs. 2 and 3). In contrast, tylvalosin pre-treatment was found to downregulate TNF-α, IL-1β, and IL-6 secretion at 4 and 24 h after LPS challenge

(Figs. 2 and 3). We believe that the tylvalosin could suppress the early and later stage of the lung inflammation. These results suggest that the protective effects of tylvalosin on LPS-induced ALI are in part attributed to inhibition of TNF-α, IL-1β, and IL-6. IL-8 (CXCL8) is a member of the CXC chemokine family, which is secreted by variety of cell types in inflammation, associated with the development and outcome of ALI/ARDS [27]. Thus, preventing the overproduction of IL-8 may attenuate lung inflammation. In this study, we found that pretreated with 50 and 100 mg/kg of tylvalosin, the IL-8 level was significantly decreased. Thus, tylvalosin has the potential for utilization in ALI.

During inflammation, large amounts of NO formed by the action of inducible nitric oxide synthase (iNOS) surpass the physiological amounts of NO usually produced by neurons nitric oxide synthase (nNOS) or endothelium nitric oxide synthase (eNOS). Furthermore, iNOS-derived NO overproduction appears to be a ubiquitous mediator of a wide range of inflammatory conditions and reflects the degree of inflammation, which represents a potential target for pharmacological intervention in inflammatory diseases [28]. Thus, the reduction in NO production has been suggested as an effective strategy for the treatment of inflammatory diseases. In this study, we shown that tylvalosin suppressed LPS dependent secretion of NO in vitro and in vivo (Fig. 2), and exhibited anti-inflammatory property, although the detailed mechanism unknown. The previous study revealed that its analogue tilmicosin exhibits potential inhibitory activity on LPS-induced NO production through suppressing the expression of inducible nitric oxide synthase (iNOS) [24]. Further work will be necessary to explore this intriguing possibility.

Like NO, prostaglandins (PGs) are well known to be important mediators of inflammation and mainly synthesized by cyclooxygenase-2 (COX-2), which is upregulated in response

to inflammatory and pro-inflammatory mediators and their products can influence many aspects of the inflammatory cascade [24]. The present study shown that the release of PGE2 was stimulated by LPS and this effect was attenuated by tylvalosin (Fig. 2). PGE2 is the most widely produced prostanoid and contributes to fever, pain and swelling during inflammation [29]. Since tilmicosin and tylosin decreased the production of PGE2 through downregulating COX-2 gene expression in vitro [24], this modulation of tylvalosin might be associated with similar effect. On the contrary, Lakritz et al. demonstrated that tilmicosin in vitro appears to reduce PGE2 production in LPS-stimulated bovine alveolar macrophages without altering COX-2 mRNA expression [30]. Therefore, unexplored regulatory mechanism for this enzyme needs to be addressed. It has been suggested that immediate production of PGE2 is mediated by cytosolic phospholipase A2 (cPLA2), and delayed production is mediated by secretory phospholipase A2-IIA (sPLA2-IIA) [31]. We hypothesized that the immunomodulating effects of tylvalosin contribute to ameliorate ALI by suppression of PLA2. It has been well established that the PLA2 is an important factor in lung diseases that involve inflammation [32]. Since this enzyme represents a family of over 30 distinct proteins with various structural and biochemical characteristics, determining the particular role of PLA2 in the setting of lung inflammation has proven quite challenging [38]. Until recently, the relationship between the role of PLA2 and the immunoregulatory effect of tylvalosin has not been elucidated.

In the present study, we found that PLA2 activity and their IHC staining (cPLA2-IVA, p-cPLA2-IVA and sPLA2-IVE) in the lung were upregulated after LPS challenge (Figs. 7 and 8). The elevation of PLA2 protein expression and activity during ALI implies its importance in this clinical setting. Based on their cellular localization, substrate specificity, and calcium-dependence, more than 30 enzymes that possess PLA2 or related activity have been identified, and they are divided into four groups: cytosolic PLA2 (cPLA2), secreted PLA2 (sPLA2) (iPLA2), calcium-independent PLA2, and lipoprotein-associated PLA2 (Lp-PLA2) [33]. The elucidation of the expression profile and biological roles of each group of PLA2s in every state of ALI/ARDS to understand which isoform(s) are the suitable targets, should be of great value for the development of therapeutic agents.

Our immunohistochemical analysis indicates that iPLA2-VI is commonly expressed in the epithelial bronchial cells, the subbronchial epithelial cells, and the leukocytes in the lungs of mice suffering from LPS challenge. However, there is no expression difference between Ctrl and ALI mice, in spite of treatment or not. Furthermore, the other studies have shown that iPLA2-VI activity in rat is unchanged with low-dose LPS infusion [34]. Thus, no evidence exists in support of a role of iPLA2-VI in ALI. It has to be pointed out that iPLA2-VIB is suggested to participate in the regulation of sPLA2-IIA expression induced by inflammatory cytokines and endotoxin [35].cPLA2s consist of six known isoforms in mammals. Among cPLA2 isoforms, cPLA2-IVA contributes to the pathogenesis of a variety of inflammation diseases [36] and has attracted attention as a target for controlling eicosanoid related inflammation. The current study was initiated to examine the potential utility of cPLA2-IVA expression as an intermediate biomarker in ALI chemoprevention trials. To this end, we examined the expression of cPLA2-IVA enzyme in the lungs from normal and LPS challenge mice treated with tylvalosin or not. As expected, cPLA2-IVA was overexpressed in the epithelial bronchial cells, subbronchial epithelial cells and in leukocytes after LPS challenge. However, tylvalosin (50 and 100 mg/kg, i.g.) treatment significantly downregulated this effect stimulated by LPS in a dose-dependent manner, followed by ALI attenuation. Thus the results of the present work put forward an enzyme (cPLA2-IVA) targeted

ALI therapy in future. Cytokines and oxidative stress are also capable of inducing cPLA2 expression in lung epithelial cells, airway smooth muscle cells, and lung fibroblasts [36]. Consequently, the cPLA2-IVA downexpression might be related with tylvalosin immunomodulation on the production of cytokines and ROS discussed above. In addition, the data that tylvalosin suppressed LPS-induced inflammatory cells recruitment and activation in mouse model also supported our conclusion, since cPLA2 plays a major role in neutrophil function in inflammatory and infectious disease clinical settings [37].cPLA2 is synthesized within the cytosol in the form of inactive enzyme and when activated, translocates to the membranes of golgi, endoplasmic reticulum and nuclear envelope in a calcium-dependent manner. Phosphorylation activation of cPLA2 on three serine residues Ser505, Ser515, and Ser727 significantly enhances its activity and represents a mechanism by which the cell regulates this enzyme's function. In this study, cPLA2-IVA phosphorylation was examined with IHC staining. As expected, LPS induced cPLA2-IVA phosphorylation, and p-cPLA2-IVA was mainly overexpressed in the epithelial bronchial cells and subbronchial epithelial cells. However, tylvalosin (50 and 100 mg/kg, i.g.) treatment significantly downregulated this phosphorylation activation in a dose-dependent manner, followed by ALI attenuation. Thus, the inhibition of cPLA2 activation may be one of the crucial protective mechanisms of tylvalosin in LPS-induced ALI. In all, inhibition of cPLA2 expression, activation and activity may diminish the formation of inflammatory mediators, resulting in reduced inflammatory manifestations, and may regulate the release of oxygen radicals that also participate in endothelial damage. Thus, this type of PLA2 may be a suitable target enzyme for the development of inhibitory therapeutic agents for the treatment of inflammatory disorders including ALI.

Accumulating evidences have indicated that some sPLA2s work in concert with cPLA2 to induce eicosanoid formation in different mammalian cells [38]. Many of sPLA2 isoforms are expressed in lung play significant roles in human inflammatory lung diseases such as ALI/ARDS, and in these conditions, elevated amounts of sPLA2 are found in the BALF and lung tissue, which seem a promising therapeutic target. Furthermore, our present study indicated that the increased expression of sPLA2-IVE colocalizes with areas of intense inflammation, and there exists a positive correlation between increased levels of sPLA2 and a poor clinical outcome. sPLA2-IVE, also known as cPLA2-ε, has been cloned from mouse tissues; however, only preliminary information is available about their biochemical properties, and nothing is known of their functional roles. Our IHC analysis further showed that it was expressed the epithelial bronchial cells, in inflammatory cells in subbronchial epithelial, and in leukocytes. To our knowledge, this is the first study showing the sPLA2-IVE expression pattern in mouse lung during ALI. The expression of sPLA2-IVE was significantly increased in the lung after LPS challenge, however, the mechanism(s) by which it increases remains unclear. Instead, tylvalosin (50 and 100 mg/kg, i.g.) treatment reversed this effect significantly. The exact role of these enzymes have not been elucidated. A better understanding of the regulation of sPLA2s levels in the plasma and BALF under normal circumstances and during ALI/ARDS will bring about superior strategies for therapeutic intervention. The involvement of sPLA2s in ALI has lead to the development of novel prodrug and liposome based drug delivery systems that are specifically activated or degraded by sPLA2s in the diseased tissue, causing a site-specific release of the associated or encapsulated drugs. The converse strategy of preventing sPLA2 activity with concomitant AA and eicosanoid generation has also been attracted attention. Conclusively, though the mechanism is obscure, the decreased activity of PLA2, the downregulation of cPLA2-IVA and sPLA2-IV expressions as well as cPLA2-IVA

activation in the lung might be one of the clues to understand the anti-inflammatory property of tylvalosin. This fact points to the PLA2 family as a potential therapeutic target for ALI.

In this study, we shown that tylvalosin was able to inhibit the replication of different PRRSV isolates (Fig. 9A), which warrants our current study in vivo. In vitro, the virus can be grown in selected simian cell lines, such as Marc-145 cells. PRRSV entry into Marc-145 cells might occur through a microfilament-dependent endocytic mechanism in which a low pH is necessary for proper virus uncoating [39]. It has been shown that tylvalosin is able to raise endosomal pH and this may be an important mechanism by which it inhibits PRRSV replication, although other factors may also be involved [20].

In our PRRSV challenge model, the severe pneumonia, characterized by a cranioventral distribution of lobular purple-colored consolidation and a diffuse tan-colored mottling of the major lung with irregular and indistinct borders, happened to piglets in nonmedication & challenge group (data not shown), which may be a potential ALI model. In agreement with the results from mice study, tylvalosin treatment attenuated piglet lung scores. In addition, PRRSV strain Hn challenge had a significant impact on BW gain, and the impact became more apparent when inspected over the longer time period after infection until 21 days p.i. (Fig. 9). In contrast, tylvalosin treatment reversed body weight drop. In this model, PRRSV challenge caused long-lasting high fever in piglet (Fig. 9), and the downmodulation of tylvalosin on rectal temperature after challenge was found. In our white Leghorns (28-day-old) fever model induced by LPS (5 mg/kg, i.p.), tylvalosin also restrained body temperature closer to normal (data not shown). These results indicate that tylvalosin seems to exhibit extensive thermoregulation in vivo. The pathogenic consequences and immunological responses of piglets to PRRSV are directly related to viral load in acute infection as reflected in viral titers in blood [40]. In the present study, tylvalosin treatment significantly reduced viral load, which might be due to its antiviral effect and rapid absorption and wide distribution properties in the tissues. These data indicate that PRRSV-induced piglet model can be used to study ALI and evaluate medicates efficacy.

To further characterize the nature of the inhibitory effect of tylvalosin on proinflammatory mediators production, ROS production, PLA2 activity and PLA2s (cPLA2-IVA, p-cPLA2-IVA and sPLA2-IVE) expression, as well as LPS and PRRS-induced lung injury, we examined the effects of tylvalosin on the activation of the NF-κB signaling pathways. The NF-κB pathway has been considered to play a pivotal role in the pathogenesis of LPS-induced ALI and PRRSV as discussed above. The heterodimers of NF-κB components, which are mostly p50/p65, are normally retained in the cytoplasm in an inactive form through being associated with an inhibitor of κB (IκB) protein [23,37]. A wide variety of stimuli can cause the phosphorylation of IκB, a process that is followed by the protein's ubiquitination and subsequent degradation. The phosphorylation induced degradation of the IκB inhibitor enables the NF-κB dimers to enter the nucleus and activate specific target gene expression [23,37]. In this study, we observed the inhibitory effects of tylvalosin on the LPS-induced NF-κB activation shown as western blot and immunohistochemical results (Figs. 10 and 11). It is reported that LPS stimulates production of reactive oxygen, elevation of PLA2s enzyme activity and activation of redox-sensitive signaling cascades including NF-κB, and then triggers elevated expression of pro-inflammatory mediators leading to acute lung injury. Our results suggested that tylvalosin reduced LPS-induced inflammation probably via inactivation of ROS and blunting the redox-sensitive inflammatory signaling NF-κB. Since NF-κB pathway plays a central role in PRRSV pathogenesis, the underlying protective mechanisms of tylvalosin in piglet is presumably the case.

In conclusion, the present study for the first time showed that tylvalosin played potent anti-inflammation and antioxidant roles in LPS, PRRSV-induced cells and animals models, which may be due to inhibition of the activation of NF-κB pathway. Tylvalosin attenuated LPS-induced inflammation and lung injury, including reduction of lung *W/D* ratio, inhibition of protein level, MPO expression and activity, and inflammatory cells aggregation in BALF. Histological examination showed that tylvalosin significantly ameliorated tissues injury with improved lung and liver morphology. Tylvalosin treatment reduced the production of proinflammatory mediators induced by LPS, the production of ROS induced by LPS and PRRSV, and the PLA2 enzyme activity. The degree of immunohistochemical staining for the cPLA2-IVA, p-cPLA2-IVA, and sPLA2-IVE was significantly reduced by tylvalosin pretreatment. Our results imply a potential role for PLA2 in the management of ALI. Furthermore, we demonstrated that tylvalosin inhibited NF-κB activation in LPS-induced ALI. In piglet model, administration of tylvalosin reversed the fluctuation of rectal temperatures to normal level, improved growth performance and reduced lung scores, which might be involved in its antiviral effect as well as the inhibition of NF-κB activation and ROS production. Therefore, tylvalosin may be considered as a potential agent for preventing ALI in the future. Also, further and comprehensive studies are needed before clinical application.

References

[1] Martin TR, Wurfel MM. A TRIFfic perspective on acute lung injury. Cell 2008;133(2):208–10.
[2] Imai Y, Kuba K, Neely GG, Yaghubian-Malhami R, Perkmann T, van Loo G, et al. Identification of oxidative stress and Toll-like receptor 4 signaling as a key pathway of acute lung injury. Cell 2008;133:235–49.
[3] Ware LB, Matthay MA. The acute respiratory distress syndrome. N Engl J Med 2000;342:1334–49.
[4] Rubenfeld GD, Caldwell E, Peabody E, Weaver J, Martin DP, Neff M, et al. Incidence and outcomes of acute lung injury. N Engl J Med 2005;353(16):1685–93.
[5] Hayes M, Curley G, Ansari B, Laffey JG. Clinical review: stem cell therapies for acute lung injury/acute respiratory distress syndrome—hope or hype? Crit Care 2012;16:205.
[6] Bhatia M, Moochhala S. Role of inflammatory mediators in the pathophysiology of acute respiratory distress syndrome. J Pathol 2004;202:145–56.
[7] Lee WL, Downey GP. Neutrophil activation and acute lung injury. Curr Opin Crit Care 2001;7:1–7.
[8] Lee JS, Frevert CW, Matute-Bello G, Wurfel MM, Wong VA, Lin SM, et al. TLR-4 pathway mediates the inflammatory response but not bacterial elimination in *E. coli* pneumonia. Am J Physiol Lung Cell Mol Physiol 2005;289:L731–8.
[9] Grommes J, Vijayan S, Drechsler M, Hartwig H, Mörgelin M, Dembinski R, et al. Simvastatin reduces endotoxin-induced acute lung injury by decreasing neutrophil recruitment and radical formation. PLoS One 2012;7(6):e38917.
[10] Tsushima K, King LS, Aggarwal NR, De Gorordo A, D'Alessio FR, Kubo K. Acute lung injury review. Intern Med 2009;48:621–30.
[11] Manicone AM. Role of the pulmonary epithelium and inflammatory signals in acute lung injury. Expert Rev Clin Immunol 2009;5:63–75.
[12] Sato K, Kadiiska MB, Ghio AJ, Corbett J, Fann YC, Holland SM, et al. In vivo lipid derived free radical formation by NADPH oxidase in acute lung induced by lipopolysaccharide: a model for ARDS. FASEB J 2002;16:1713–20.
[13] Clark SC, Sudarshan CD, Khanna R, Roughan JV, Flecknell PA, Dark JH. A new porcine model of reperfusion injury after lung transplantation. Lab Anim 1999;33(2):135–42.
[14] Gehrke I, Pabst R. Cell composition and lymphocyte subsets in the bronchoalveolar lavage of normal pigs of different ages in comparison with germ-free and pneumonic pigs. Lung 1990;168:79–92.

[15] Mazzola S, Forni M, Albertini M, Bacci ML, Zannoni A, Gentilini F, et al. Carbon monoxide pretreatment prevents respiratory derangement and ameliorates hyperacute endotoxic shock in pigs. FASEB J 2005;19(14):2045–7.

[16] Chang RJ, Trible BR, Rowland RR. Pathogenesis of porcine reproductive and respiratory syndrome virus. Curr Opin Virol 2012;2:256–63.

[17] Mateu E, Diaz I. The challenge of PRRS immunology. Vet J 2008;177:345–51.

[18] Martínez-Lobo FJ, Díez-Fuertes F, Segalés J, García Artiga C, Simarro I, Castro JM, et al. Comparative pathogenicity of type 1 and type 2 isolates of porcine reproductive and respiratory syndrome virus (PRRSV) in a young pig infection model. Vet Microbiol 2011;154(1–2):58–68.

[19] Stuart AD, Brown TDK, Imrie G, Tasker JB, Mockett APA. Intracellular accumulation and trans-epithelial transport of aivlosin, tylosin and tilmicosin. Pig J 2007;60:26–35.

[20] Stuart AD, Brown TDK, Mockett APA. Tylvalosin, a macrolide antibiotic, inhibits the in vitro replication of European and American porcine reproductive and respiratory syndrome virus (PRRS) viruses. Pig J 2008;61:42–8.

[21] Halbur PG, Paul PS, Frey ML, Landgraf J, Eenisse K, Meng XJ, et al. Comparison of the pathogenicity of two US porcine reproductive and respiratory syndrome virus isolates with that of the Lelystad virus. Vet Pathol 1995;32:648–60.

[22] Menegazzi M, Di Paola R, Mazzon E, Muica C, Genovese T, Crisafulli C, et al. Hypericum perforatum attenuates the development of carrageenan-induced lung injury in mice. Free Radic Biol Med 2006;40:740–53.

[23] Lee SM, Kleiboeker SB. Porcine arterivirus activates the NF-kappaB pathway through IkappaB degradation. Virology 2005;342:47–59.

[24] Cao XY, Dong M, Shen JZ, Wu BB, Wu CM, Du XD, et al. Tilmicosin and tylosin have anti-inflammatory properties via modulation of COX-2 and iNOS gene expression and production of cytokines in LPS-induced macrophages and monocytes. Int J Antimicrob Agents 2006;27:431–43.

[25] Laskin DL, Pendino KJ. Macrophages and inflammatory mediators in tissue injury. Annu Rev Pharmacol Toxicol 1995;35:655–77.

[26] Lee IT, Yang CM. Role of NADPH oxidase/ROS in pro-inflammatory mediators-induced airway and pulmonary diseases. Biochem Pharmacol 2012;84(5):581–90.

[27] Kurdowska A, Noble JM, Steinberg KP, Ruzinski JT, Hudson LD, Martin TR. Antiinterleukin 8 autoantibody: interleukin 8 complexes in the acute respiratory distress syndrome–relationship between the complexes and clinical disease activity. Am J Respir Crit Care 2001;163:463–8.

[28] Clancy RM, Amin AR, Abramson SB. The role of nitric oxide in inflammation and immunity. Arthritis Rheum 1998;41:1141–51.

[29] Steiner AA, Ivanov AI, Serrats J, Hosokawa H, Phayre AN, Robbins JR, et al. Cellular and molecular bases of the initiation of fever. PLoS Biol 2006;4(9):e284.

[30] Lakritz J, Tyler JW, Marsh AE, Romesburg-Cockrell M, Smith K, Holle JM. Tilmicosin reduces lipopolysaccharide-stimulated bovine alveolar macrophage prostaglandin E(2) production via a mechanism involving phospholipases. Vet Ther 2002;3:7–21.

[31] Kudo I, Murakami M. Phospholipase A2 enzymes. Prostaglandins Other Lipid Mediat 2002;68–69:3–58.

[32] Suzuki N, Ishizaki J, Yokota Y, Higashino K, Ono T, Ikeda M, et al. Structures, enzymatic properties, and expression of novel human and mouse secretory phospholipases A2. J Biol Chem 2000;275:5785–93.

[33] Murakami M, Sato H, Taketomi Y, Yamamoto K. Integrated lipidomics in the secreted phospholipase A2 biology. Int J Mol Sci 2011;12(3):1474–95.

[34] Kellom M, Basselin M, Keleshian VL, Chen M, Rapoport SI, Rao JS. Dose-dependent changes in neuroinflammatory and arachidonic acid cascade markers with synaptic marker loss in rat lipopolysaccharide infusion model of neuroinflammation. BMC Neurosci 2012;13:50.

[35] Kuwata H, Fujimoto C, Yoda E, Shimbara S, Nakatani Y, Hara S, et al. A novel role of group VIB calcium-independent phospholipase A2 (iPLA2) in the inducible expression of group IIA secretory PLA2 in rat fibroblastic cells. J Biol Chem 2007;282:20124–32.

[36] Ghosh M, Tucker DE, Burchett SA, Leslie CC. Properties of the Group IV phospholipase A2 family. Prog Lipid Res 2006;45:487–510.

[37] Levy R, Dana R, Hazan I, Levy I, Weber G, Smoliakov R, et al. Elevated cytosolic phospholipase A2 expression and activity in human neutrophils during sepsis. Blood 2000;95(2):660–5.

[38] Muñoz NM, Kim YJ, Meliton AY, Kim KP, Han SK, Boetticher E, et al. Human group V phospholipase A2 induces group IVA phospholipase A2-independent cysteinyl leukotriene synthesis in human eosinophils. J Biol Chem 2003;278(40):38813–20.

[39] Kreutz LC, Ackermann MR. Porcine reproductive and respiratory syndrome virus enters cells through a low pH-dependent endocytic pathway. Virus Res 1996;42(1–2):137–47.

[40] Johnson W, Roof M, Vaughn E, Christopher-Hennings J, Johnson CR, Murtaugh MP. Pathogenic and humoral immune responses to porcine reproductive and respiratory syndrome virus (PRRSV) are related to viral load in acute infection. Vet Immunol Immunopathol 2004;102:233–47.